JOURNAL OF Materials CHEMISTRY

A scanning probe study of some short chain self-assembled alkylsilane films

Jingxin Li and J. Hugh Horton*

Department of Chemistry, Queen's University, Kingston, Ontario, Canada K7L 3N6. E-mail: hortonj@chem.queensu.ca; Fax: +1-(613)-533-6669; Tel: +1-(613)-533-2379

Received 13th November 2001, Accepted 18th February 2002
First published as an Advance Article on the web 20th March 2002

Trichloroalkylsilanes readily form self-assembled monolayers (SAMs) on mica surfaces. The present work uses scanning probe methods (atomic force microscopy (AFM), chemical force microscopy (CFM) and nanoindentation) to study aspects of the assembly process and the properties of some short chain forms of these self-assembled monolayers. The deposition of propyltrichlorosilane ($CH_3CH_2CH_2SiCl_3$, PTS) and allyltrichlorosilane ($H_2C{=}CHCH_2SiCl_3$, ATS) at varying temperatures (−78 °C to +25 °C) on mica substrates has been examined. The ATS films were subsequently modified by oxidation to form a –COOH terminated species. These films were characterized by chemical force microscopy using functionalized tips at varying pH values. In addition, nanoindentation was utilized to study the Young's modulus and hardness of the films. We find that at low deposition temperatures, smooth overlayers of these short chain films are formed, without the formation of polymerised aggregates that are seen at higher temperatures. The surface ordering also appears to be higher under these conditions. The surface pK_a of the oxidized ATS is larger than that of the longer chain analogue previously characterised by chemical force microscopy. Nanoindentation can readily distinguish between ordered and polymerised aggregates on the surface.

Introduction

Self-assembled monolayers (SAMs) such as alkyltrichlorosilanes of the form $CH_3(CH_2)_nSiCl_3$ have attracted considerable attention due to their potential technological applications.[1–6] Basically, these films consists of a hydrocarbon chain covalently attached to the surface *via* an Si–O bond, which makes the longer chain systems good models of the lipid membrane of a cell. These films are also effective at adsorbing small molecules from solution and thus can be used to analyze trace amounts of carcinogenic molecules such as polycyclic aromatic hydrocarbons (PAHs) in water supplies. They are also similar to the structures seen on the adsorbent phase in chromatography columns, thus making them a good model for exploring the mechanism of chromatographic separation. In these latter applications, the chain length of the film, and the relative surface ordering can have a considerable effect on the adsorption kinetics and selectivity of these films for molecules in solution. Thus, further exploration of the effects of chain length on the surface structure is warranted.

Long chain alkyltrichorosilanes ($n \geqslant 10$) have been successfully constructed on several substrates such as mica[7–9] and silicon (in effect on the SiO_2 overlayer).[10–11] Previous workers have found that on Si the critical transition temperature, T_c, for film ordering of the deposited *n*-alkyltrichlorosilanes is highly dependent on the chain length.[12] Above T_c, the films are disordered and characterised by higher surface energy as determined by contact angle measurements. They are also characterised by the presence of agglomerated regions of polymerised alkylsilanes deposited on the surface, leading to a less smooth and continuous overlayer. The transition temperature on silicon ranges from 0 °C for $n = 10$ to 38 °C for $n = 22$ and shifts 3.5 ± 0.5 °C per additional methylene group in the grafted chain on silicon substrate. The critical temperature should be expected to be much lower for short chain systems. On mica, alkyltrichlorosilanes deposit by a similar mechanism to that on Si, but are bound at fewer surface sites and hence exhibit a higher degree of cross-linking and lower surface ordering. Nonetheless, monolayers of long chain alkyltrichlorosilanes such as octadecyltrichlorosilane (OTS) may be formed, as determined by AFM measurements. However, an examination of temperature effects on the deposition of these films, and particularly on the shorter chain alkyltrichlorosilanes has not been carried out. Therefore, we have chosen to focus here on the deposition of short chain alkylsilanes propyltrichlorosilane (PTS) and allyltrichlorosilane (ATS) to examine this critical deposition temperature phenomenon further on the mica substrate. ATS is particularly interesting to examine as the double bond at the end of this chain may undergo further reaction to form a variety of functional group terminations.

The effects of both deposition temperature and reaction time on the surface topography will first be examined by AFM imaging. The surface ordering of self-assembled films of ATS and PTS will then be examined by measuring the mechanical properties (hardness and Young's modulus) of the films using nanoindentation techniques.[13–17] Under moderately low temperature conditions, topographically smooth films are indeed found to form on the surface. However, polymerised regions may be found on these films, and we show how the mechanical properties of the films allow us to distinguish these from the smoother regions using indentation methods. The surface structure is further explored by examining chemically modified films, produced by oxidation of the double bond in ATS to form a –COOH terminated surface. These are studied using chemical force microscopy (CFM) methods. In this technique force microscope probe tips are modified by covalent linked organic monolayers that terminate in well-defined functional groups. This enables direct probing of adhesion forces between the distinct functional groups on the tip and sample as a function of pH, allowing the surface pK_a to be determined. The surface pK_a and the titration curve shape are in turn compared to measured and previously calculated values for various similar systems.

 DOI: 10.1039/b110353a

Experimental

Sample preparation

Mica substrates were activated for alkylsilane deposition by exchanging H^+ for alkali ions on the mica surface, according to the method of Carson and Granick.[18] Grade 5 research quality miscovite mica squares (SPI supplies, West Chester, Pennsylvania) were cut into rectangles (1.4 × 1.8 cm). Both sides of the samples were cleaved. They were mounted vertically in a glass holder to allow for uniform exposure of a 0.50 M HCl solution to both surfaces of the mica sample slides. After a three-hour exposure to the HCl solution, the slides were removed, dried at 0.1 Torr N_2 in a dessicator for 30 minutes and stored under an N_2 atmosphere.

Glassware used in the subsequent deposition process was passivated towards alkylsilane deposition by exposing it to 10% to 15% by volume concentrations of OTS in dry toluene for a period of 24 hours. Allyltrichlorosilane (95%, Aldrich) and propyltrichlorosilane (95%, Aldrich) were deposited on the mica substrates by exposing the slides to 6.0×10^{-3} M solutions of the appropriate compound in petroleum ether for periods of 10–120 minutes. Petroleum ether was used as a solvent here instead of the more usual cyclohexane mixtures as it has a freezing point below the −78 °C used in some of the deposition experiments. The deposition process took place under a dry nitrogen atmosphere to minimize the effect of water vapour on the formation of polymers in the monolayers. Depositions at 0 °C and −78 °C were carried out with the reaction vessel cooled by a water–ice or dry ice–acetone bath respectively. Following deposition, the samples were removed from the silane solutions and then stored in a desiccator under dry nitrogen.

The ATS films were further modified to the corresponding hydroxy termination *via* a permanganate–periodate oxidation process. First, stock solutions of $KMnO_4$ (5 mM), $NaIO_4$ (195 mM), and K_2CO_3 (18 mM) in water were prepared. Immediately prior to the oxidation, 1 mL from each of these solutions was combined with 7 mL of distilled water to create the oxidizing solution ($KMnO_4$, 0.5 mM, $NaIO_4$, 19.5 mM, K_2CO_3, 1.8 mM, pH 7.5).[19] The ATS monolayers were placed in the sample holder and exposed to this solution for a 24 hour period. Subsequently, the samples were removed from the solution and rinsed in sequence in 20 mL each of $NaHSO_3$ (0.3 M), water, 0.1 M HCl, water and ethanol. The samples were then dried under a flow of nitrogen and stored in a desiccator under dry nitrogen for future use.

Instrumental analysis

Deposition of alkylsilanes on the mica substrate was confirmed from FTIR-ATR spectra by the presence of absorptions at 2921 cm^{-1} and 2851 cm^{-1} due to CH_2 stretches. These were acquired using a Nicolet Avatar 360 E. S. P. FT-IR Spectrometer (Madison, Wisconsin, USA). The AFM used was a Pico SPM (Molecular Imaging: Phoenix, Arizona) with Nanoscope E software and electronic interface (version 4.22: Digital Instruments: Santa Barbara, California). Images were acquired in contact mode using standard Si_3N_4 tips under aqueous solution. For the chemical force microscope experiments, standard Si_3N_4 contact mode tips were coated with a 200–250 Å layer of gold and subsequently immersed for 48 h in a 1.0×10^{-3} mol L^{-1} solution in methanol of 16-thiohexadecanoic acid to produce –COOH terminated tips. For the acquisition of force curves, the CFM tips and samples were immersed in freshly prepared unbuffered aqueous NaOH or HCl solutions of pH ranging from 3–10. Ionic strength was held constant at 10^{-3} mol L^{-1} by adjusting with appropriate concentrations of NaCl. The pH of the solutions was checked before and after the experimental run to ensure that the pH had not changed. Some 300–500 force curves were obtained for each sample. Experimental runs for a single pH series were performed using a single tip on a given sample. The runs were then repeated on three different samples. The reported values of the adhesive interaction are an average of all the curves while the reported errors reflect the standard deviation of the data.

The nanoindentator used in this project was a Hysitron Tribscope used in conjunction with the AFM system described previously. (Hysitron Inc., Minneapolis, MN, USA). The force range of the Triboscope is 1 μN to 10 mN with 100 nN sensitivity, while the displacement range is 5 μm full scale with 0.2 nm sensitivity. The Berkovich diamond tip used in the nanoindentation experiments was calibrated based on a determination of the tip area function according to the method provided by Oliver and Pharr.[15] This method is based on the assumption that the Young's modulus of the calibration material is independent of indentation depth. Here, fused quartz with a reduced Young's modulus of 69.6 GPa was used as the standard sample for calibration.

Results and discussion

AFM imaging

Self-assembled monolayers of ATS and PTS film were deposited under a variety of conditions on mica substrates. Fig. 1a shows a 12.37 μm × 12.37 μm AFM image of PTS deposited on mica after 10 min at room temperature (25 °C). Polymerized aggregates are found scattered randomly on the mica surface. Cross section analysis revealed that the diameters of the agglomerates range from 0.7 μm to 3.3 μm with an approximate density of 0.65 aggregate per μm^2. Typically, the height of these agglomerates ranged from 6 nm to 22 nm.

In order to reduce the density of the polymerized features, subsequent experiments were carried out at lower temperatures. Fig. 1b shows a 9.315 μm × 9.315 μm AFM image of PTS deposited on mica after 10 minutes at 0 °C. Three types of features may be observed. First, small polymerized aggregates were still found scattered on the mica surface, but compared to a sample of similar size at room temperature (Fig. 1a), both the size and the density of the aggregates are much reduced. Instead, we see small, ring-like regions with a small depression in the centre. Such features are observed more clearly as the exposure time is increased (below). The remaining features are high and low plateau regions of the films, which are both relatively flat. Mean roughness as obtained by roughness analysis was 3.9 nm for the higher regions of the surface. For the lower area, the value was 0.64 nm. This is similar to that found for a bare mica surface, indicating that these regions remained unreacted.

Cross-section analysis was performed on several images (Fig. 1b). This showed that the estimated vertical displacement between the overlayer and the bare mica regions, which should correspond to the thickness of the overlayer, range from 6.8 nm to 10 nm. Taking into account that an average C–C single bond is 1.54 Å in length, the expected chain length of a PTS molecule would be 4.62 Å. It may be concluded that 10–20 overlayers of PTS have been formed. Thus, we may conclude that under these conditions the film formed is relatively disordered, consisting of a cross-linked overlayer some 10–20 molecules thick. However, the density of the aggregate features is significantly reduced under these conditions.

Further experiments were carried out on the PTS films at longer deposition times. Fig. 1c shows a 20 μm × 20 μm AFM image of PTS deposited on mica after 30 minutes at 0 °C. The ring features, observed at the lower deposition time, are now particularly evident. The protruding vertical wall of the ring is about 10 nm higher than the surface of the SAM layer. The further evolution of these features at longer deposition times may be seen in Fig. 1d which shows a 20 μm × 20 μm AFM image of PTS deposited on mica after 60 minutes at 0 °C. The

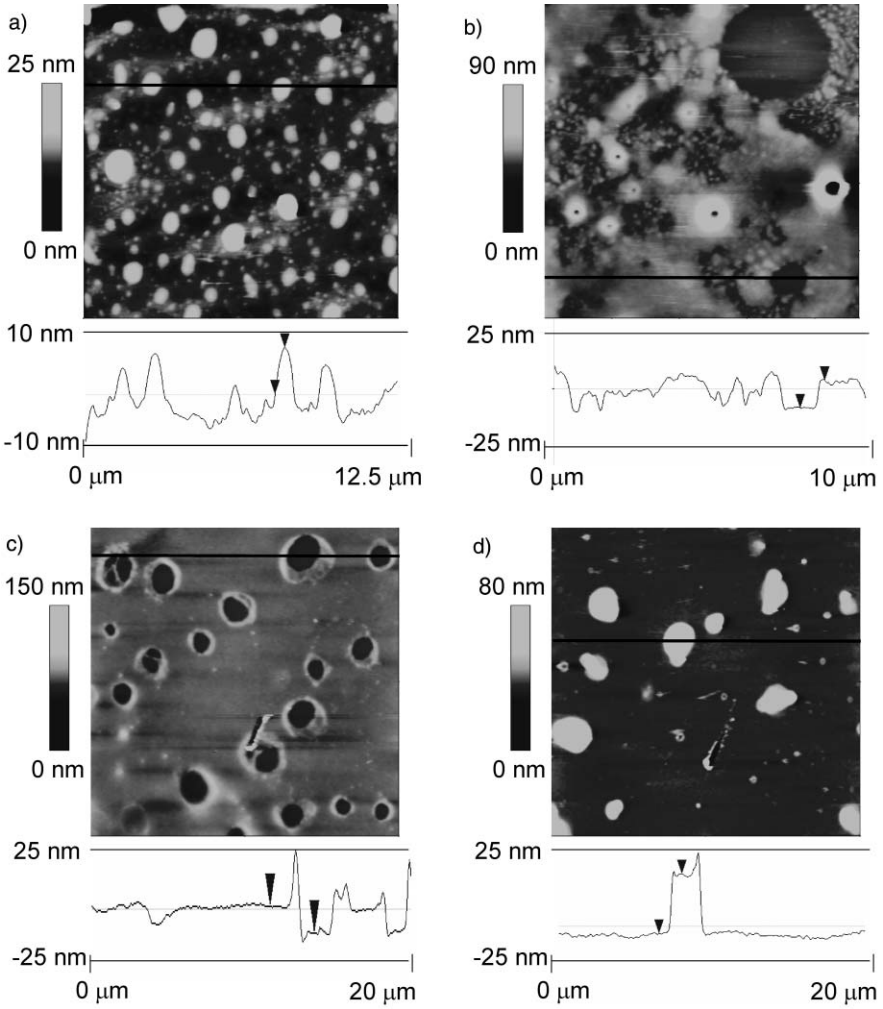

Fig. 1 AFM images of propyltrichlorosilane deposited on mica under various conditions: (a) deposited at 25 °C for 10 minutes (scan scale: 12.37 μm × 12.37 μm). Under these conditions, polymerized aggregates are deposited on the surface and the film quality is poor. (b) deposited at 0 °C for 10 minutes (scan scale: 9.315 μm × 9.315 μm). Fewer aggregates are deposited on the surface and a discontinuous film of PTS if formed. There are numerous ring-shaped features and regions of bare mica. As the deposition time is increased under the same temperature conditions in (c) to 30 minutes (scan scale: 20 μm × 20 μm) the bare regions are filled in and the rings become more distinct and finally in (d) after 60 minutes deposition (scan scale: 20 μm × 20 μm) the ring features are entirely filled in and the surface is coated with layer some 20 PTS molecules thick.

surface is generally flat after this extensive deposition period except for some plateaus, 21–40 nm high, which arise from the filling-in of the ring-like features seen at lower deposition time. These features may represent nucleation of the PTS taking place at a higher rate near defect sites on the film, or alternatively, could be micelles of PTS formed in solution which have subsequently settled onto the surface. Significantly, in the plateau region outside these rings, the film thickness has increased continually with deposition time. While a smooth film of PTS is being formed, as opposed to the aggregate features at higher temperatures, it remains reactive and continues to cross link with unreacted alkylsilanes in solution to form a disordered overlayer on the surface.

A similar series of deposition experiments were carried out using ATS. Fig. 2 shows an AFM image of ATS deposited on mica after 10 minutes at 0 °C. A homogeneous and fairly continuous overlayer is observed. The largest vertical displacement obtained here is 2.0 nm, which is considerably smaller than the value obtained on the PTS samples and indicates that the film is only three to four molecules thick. Compared to PTS samples formed under the same conditions, a much more ordered layer was formed. Such a film thickness is similar to that for the much longer chain OTS deposited on mica[20] at 298 K, although in that case the layer was only 1–2 molecules thick.

Samples exposed to the ATS solution for longer times (20 to 60 minutes) reveal much the same periodic ordering and cross-linking network as seen in Fig. 2. Significantly, the overlayer thickness does not increase with deposition time, unlike the case of the PTS film, indicating that the deposition process has terminated with a 3–4 layer film. There is a

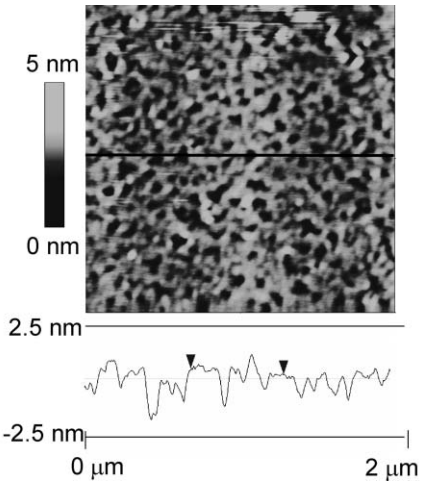

Fig. 2 AFM image of allyltrichlorosilane deposited on mica at 0 °C for 10 minutes (scale: 1.996 μm × 1.996 μm). A homogeneous film some 3–4 molecules thick is formed under these conditions.

considerable improvement in film quality compared to those deposited at room temperature, indicating that lower temperatures lead to improvements in film ordering, and certainly smoothness for ATS.

Deposition of ATS at a lower temperature (−78 °C) was also carried out to determine if more ordered films could be formed. However, the polymerized aggregates which seemed to have almost disappeared at 0 °C, emerge again and are found scattered randomly on the mica surface. These agglomerates resemble the features seen on PTS samples at room temperature. The most likely explanation is that polymer features found at −78 °C are due to water condensing within the reaction vessel at the low temperature used for this reaction, despite the precautions taken to prevent this occurrence by carrying out the process under nitrogen.

While deposition at very low temperatures was not successful it is clear that, as indicated by both the topography and film thickness, a much smoother and thinner layer was observed when depositing ATS SAMs at a temperature of 0 °C compared to the PTS films. While ATS (allyltrichlorosilane) and PTS (propyltrichlorosilane) contain the same length of carbon chain, the double bond at the end of the ATS chain should lead to a higher degree of steric hindrance. This will prevent the access of unreacted silanes from solution to the reactive Si–Cl centres, thereby reducing the establishment of silane cross-linking and hence restrict the growth of the films.

Nanoindentation

In Fig. 1 aggregate particles and ring-like, presumably polymerised, features appear scattered on the surface. One question that may arise is the formation mechanism of these features. Were they formed directly on the surface or did they first form in the solution and then settle onto the surface? In the former case, they should be bonded directly through Si–O linkages and hard to remove. In the latter case, they will only be weakly held and should be readily removed mechanically.

Fig. 3, parts (a) and (b), shows two 2 μm × 2 μm AFM images of ATS deposited on mica for 10 minutes at −78 °C. As noted previously, deposition under these conditions also gave rise to polymer aggregates similar to those seen in Fig. 1. Unlike the images seen in Figs. 1 and 2, acquired using a standard Si_3N_4 tip, those in Fig. 3 were acquired using the nanoindentator with a diamond tip. This tip was used during the nanoindentation experiments and is blunter than a standard Si_3N_4 tip, leading to poorer image quality. During an indentation experiment, it is normal practice to move the tip to the centre of the intended target position before carrying out the actual indentation, and then image the indent region. In Fig. 3(a) and (b), the white circle indicates a large polymer feature that was removed from the surface during the scanning process but before any indentation process took place. Since the image quality degrades somewhat after the change, we may conclude that the polymer feature has been transferred to the tip, changing its imaging properties. In the region where the polymer used to reside, a residue layer can still be seen in Fig. 3b. This phenomenon was often found while performing tip manoeuvres. Such a phenomenon could be readily distinguished from the process observed during an indent cycle, where the aggregate remained on the surface and the usual triangular depression associated with the indent process was observed, as can be seen in parts (c) and (d) of Fig. 3. All these images were taken at a force setpoint of 2 nN. Under these low force set point conditions the ATS film surrounding the aggregates, or indeed the residue regions, was not removed or damaged, demonstrating that these features are more strongly bound to the surface. Indeed, it took a force in excess of 20 nN to effect further surface damage to the films. Similar forces have been previously used to effect the removal of ordered OTS films on mica,[20] where the alkylsilane film was shown to be attached through only occasional Si–O linkages to the surface. These observations are strong evidence to indicate that instead of forming directly on the surface, these aggregate features, unlike the layered regions, are merely physisorbed on the surface. Instead they were formed in the solution first and then settled onto the surface.

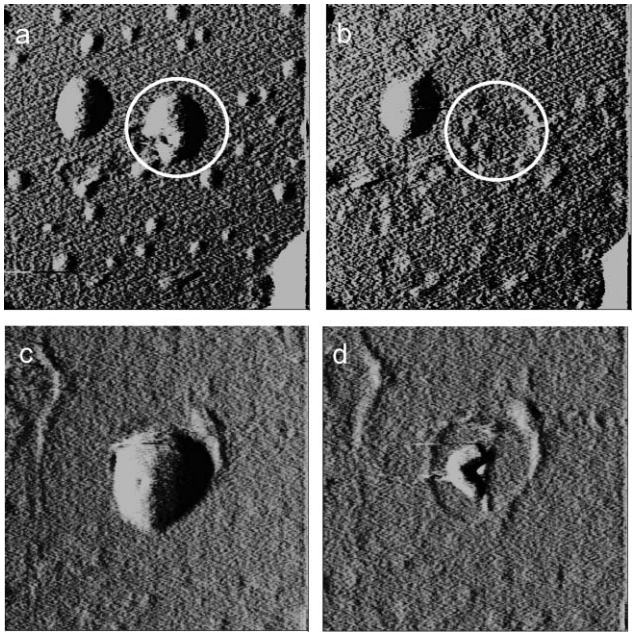

Fig. 3 AFM images of allyltrichlorosilane deposited on mica at −78 °C for 10 minutes (all scales: 2 μm × 2 μm). Images (a) and (b) were acquired during scanning but before the nanoindentation process took place. They were acquired at a force setpoint of 2 nN before and after positioning the tip over the indent site. The circle indicates the aggregate feature that has been removed from the surface during the scan, leaving a residue region exposed below. Scanning under these conditions did not damage the smoother regions of the film. The two lower images were taken at the same setpoint of 2 nN and show an aggregate feature immediately (c) before and (d) after indentation took place on the sample at a maximum load of 10 μN. Note the triangular indent region left in the surface surrounded by residual alkylsilane.

This may be further checked by indentation experiments on the various surface features of the film. Using the method of Pharr and Oliver,[15] load-indent displacement curves were analysed for indents acquired on the layered (or plateau) regions of the films, the aggregate regions, and areas where a residue was left after removal of the aggregate by the tip. The resulting average Young's modulus and hardness value are listed in Table 1. Note that the Young's moduli are all lower than that obtained for a clean mica substrate. The number of measurements for layer, residue and aggregate regions were 10, 9 and 7, respectively. The values reported are those observed at indent depths above 10 nm. At indent depths below this, the Young's modulus and hardness are variable, and slowly increase before saturating at indent depths above 10 nm. In an overlayer film/substrate system such as that examined here, the values obtained do not represent the modulus and hardness of the film alone, but rather depend on the properties of both.

Table 1 Young's modulus and hardness values determined for various film features for the allyltrichlorosilane films deposited on mica. Features are explained in the text

Features	Young's Modulus/GPa	Hardness/GPa
Layer	51.3 ± 1.4	5.3 ± 0.4
Residue	52.3 ± 1.4	5.5 ± 0.2
Polymer	44.4 ± 4.5	3.7 ± 0.9
Mica (published)	59.9 ± 2[a]	5.0 ± 0.1

[a]See Ref. 24, 25.

At indent depths less than the overlayer thickness, the Young's modulus and hardness are a strong function of indent depth.[16] As the indent depth becomes comparable to the film thickness they plateau at values intermediate to those of the pure film and substrate.

While the values obtained do not represent the absolute values for Young's modulus and hardness of the films, a comparison of the values in Table 1 shows that the layer and residue regions are indistinguishable within experimental error. The polymerised regions have lower Young's modulus and hardness values than the layered or residue regions: this certainly is what we might expect as a disordered polymer layer should be more compliant than an alkylsilane overlayer. This is strong evidence that while removal of the polymer particle did occur, a residue of ATS, adsorbed before the polymer particle settled, remains behind on the surface. All the regions show a lower Young's modulus and hardness than the mica substrate itself.

Chemical force microscopy: force titration curves

The ATS films were oxidized in order to form carboxylate functional groups on the surface. The results of chemical force titration measurements on these surfaces using a tip terminated with 16-thiohexadecanoic acid are shown in the upper graph of Fig. 4. Data were acquired on a) the unmodified ATS surface and b) an ATS surface oxidized to form a –COOH end group. It is clear that the adhesion forces depend on the chemical identity of the sample surface and are also highly sensitive to changes in solution pH. In either case, adhesion forces are generally found to decrease with increasing pH of the solution. However, in the case of the unmodified ATS surface, the adhesion force drops constantly with increasing pH, while on the oxidized ATS surface, we see a maximum in the adhesive interaction at a pH of 4, followed by a rapid decrease at pH values greater than 6. The magnitude of the forces observed (maximum 18 nN) on the unmodified ATS surface is also relatively smaller compared to the oxidized case.

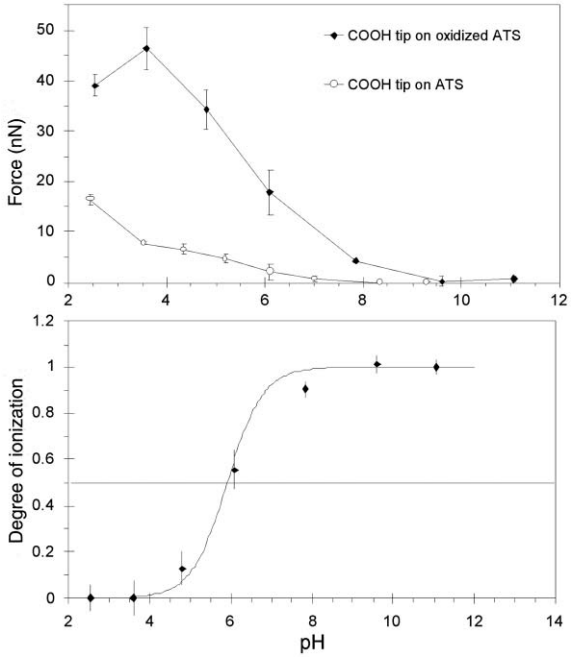

Fig. 4 Adhesion force titration curves recorded in solution. The upper graph shows adhesion force *versus* pH using a tip terminated in 16-thiohexadecanoic acid on (filled squares) an as-deposited allyltrichlorosilane film and (open circles) on an allyltrichlorosilane film oxidized to produce a –COOH terminal group. The lower graph shows the degree of ionization (see text) of the oxidized allyltrichlorosilane film–thiohexadecanoic tip system as a function of pH. The dotted line shows the degree of ionization of a weak acid of pK_a 5.9 in solution.

To account for these effects, the chemical identity of the tip and sample surface and also the changes in the ionization state of the end groups must be considered. In both cases, the end groups on the tip are the same. At low pH, the tip is terminated with uncharged COOH groups. At high pH, the COOH group is deprotonated and negatively charged COO^- is formed. The pK_a of the acid group for a long chain carboxylic acid in solution, such as the 16-thiohexadecanoic acid used here, is generally quoted as 4.8. However, previous workers have found that in the case of self-assembled monolayers of COOH-terminated thiols, this value is shifted upwards to about 5.2–5.5, due to the difficulty in solvating the end groups on the surface.[21,22]

The observed decrease in adhesive force with increasing pH must be attributed to electrostatic repulsion between negatively charged carboxylate groups on the tip and some negatively charged group on the surface. This reduction in adhesive interaction, as might be expected, starts at pH values similar to the pK_a of the tip. In the case of unmodified ATS however, the end group on the surface is an unsaturated hydrocarbon and there is no ionizable group present. The repulsive interaction may come from two sources: either preferential adsorption of OH^- or some other negative counter ion on the surface with increasing pH, or ionization of bare regions of mica substrate that have been left unreacted. Since the AFM images on these samples show no uncovered regions, the former explanation seems more likely. The relatively smaller magnitude of the adhesive interaction is observed here because there is no possibility of forming a strong hydrogen-bond interaction, as will be the case in the COOH–oxidized ATS system.

In the case of the oxidized ATS sample, the analysis can be made much more quantitative. Here, the unsaturated hydrocarbon surface was oxidized by $KMnO_4$ and $NaIO_4$ during the modification process to become a –COOH end group. These may also be deprotonated at high pH. Therefore, the adhesive interaction at low pH values originates from hydrogen bonding between uncharged COOH groups. The maximum adhesive interaction observed here at a pH of 4, should occur near the pK_a of the tip and the sample. At this point, with half the sites ionized on both tip and sample, maximum H-bonding should occur. With the increase of pH, the decrease in adhesive force at pH $>$ 6 can be attributed to electrostatic repulsion between negatively charged carboxylate groups on both the tip and sample. The force-*versus*-separation shows essentially little adhesion at pH $>$ 7, indicating that the surface charge density is saturated under these conditions, *i.e.* the carboxy groups are fully deprotonated.

This result is comparable to the result of Vezenov *et. al.*,[22] who reported similar results for tips and samples terminated with 16-thiohexadecanoic acid, in which a maximum was observed at a pK_a of 5.5 $\pm$ 0.5. In that case, both tip and sample were coated with the same alkanoic acid. In our case, the maximum must correspond to some average pK_a of tip and sample. van der Vegte and Hadziioannou[21] have proposed an analysis method to determine the pK_a of an alkanoic acid surface using tips and samples coated with 11-thioundecanoic acid, and found that the surface pK_a of this species was 5.2 based on a determination of the degree of ionization, α, values of the surface functional groups. This is given by the equation

$$\alpha[\mathrm{pH}(x)] = \frac{F_{adh}[\mathrm{pH(min)}] - F_{adh}[\mathrm{pH}(x)]}{F_{adh}[\mathrm{pH(min)}] - F_{adh}[\mathrm{pH(max)}]} \quad (1)$$

where $F_{adh}[pH(min)]$ and $F_{adh}[pH(max)]$ represent the adhesive forces observed at the minimum and maximum extremes of pH respectively. The force data can thus be replotted as degree of ionization data in the lower graph of Fig. 4 for our tip–sample system. On the same graph, the distribution curve showing the degree of ionization for a weak acid with a pK_a of 5.9 is also shown. As can be seen, our adhesion data are consistent with

an effective pK_a of about 5.9. In fact, the effective pK_a of a surface ionizable group, unlike a molecule in solution, tends to increase with increasing pH, since as surface sites are deprotonated, it becomes increasingly difficult to ionize adjacent to negatively charged, previously ionized sites. The effective pK_a of the system can in fact be calculated as a function of pH using the equation

$$pK_{eff} = pH - \log\frac{\alpha}{1-\alpha} \quad (2)$$

Using eqn. (2), we find pK_a values for the tip sample combination ranging from 5.6 at a pH of 4.2 to a pK_a of 6.8 at a pH of 9.6, but with an average pK_a value of 5.9. This value is higher than that previously determined (5.2) for an undecanoic acid tip–sample system.[21] Indeed, when it is considered that the value measured is an average for the tip–sample combination, it seems likely that the pK_a of the three-carbon alkanoic acid surface is somewhat higher. The force–pH curve profile seen here is very similar to that observed[23] for a 11-thioundecanoic acid tip titrated against a 3-thiopropanoic acid monolayer deposited on Au, except that the sigmoidal region is shifted approximately 2 pH units higher due to the very low ionic strength (10^{-7} mol L^{-1}) conditions used in that work. The sigmoidal shape observed is characteristic of a system which has a mixed hydrophobic–hydrophilic interaction, as a result of exposed alkyl spacer groups at the surface. This then indicates that the ATS films were not completely ordered, which is consistent with the AFM imaging which demonstrated a four layer thick film had been deposited on the surface.

Conclusions

Self-assembled monolayers of propyltrichlorosilane and allyltrichlorosilane were deposited at varying temperatures (−78 °C to 25 °C) on mica surfaces. AFM was used to study aspects of the assembly process and properties of these self-assembled monolayers. We found that these short chain alkylsilanes formed smooth films only at temperatures below 0 °C. Room temperature deposition led to the formation of large numbers of unstructured aggregate forms on the surface. Aggregate features were present on the PTS films under all conditions, but at lower temperatures they appeared to arise either due to nucleation at defect sites on the surface, or as micelles of polymerised alkylsilane which settled on the surface to form distinct ring-like features. Ring features were not observed in the films of ATS, and they were more ordered than the corresponding PTS films, as indicated by film thickness measurements.

The unstructured aggregate features were relatively easy to remove from the surface using a diamond tip used for nanoindentation studies of the films. Nanoindentation measurements showed that the Young's modulus and hardness could distinguish the layered PTS regions of the film and the aggregate features. As might be expected for a polymerised alkylsilane, both the Young's modulus and hardness of the aggregate features were smaller than those of the more highly ordered layered regions of the film. Residue regions that originally lay underneath the aggregate features that had been removed with the tip, had Young's modulus and hardness values that were indistinguishable from the layered regions of the film. These observations suggest that the aggregate particles formed in solution and settled onto the surface after the alkylsilane film had formed.

Chemical force titrations were used to characterize both the as-deposited ATS films and those which had undergone oxidation to form a carboxylate terminated end group. The force titration results were consistent with previous pK_a measurements of longer chain alkylthiol films deposited on Au, though the measured pK_a of 5.9 was higher than those previously reported, but the titration curve profile indicated that the film was still disordered.

Acknowledgement

We acknowledge the Natural Sciences and Engineering Research Council of Canada for financial support.

References

1 P. E. Laibinis, J. J. Hickman, M. S. Wrighton and G. M. Whitesides, *Science*, 1989, **245**, 845.
2 A. Kumar and G. M. Whitesides, *Science*, 1994, **263**, 60.
3 K. L. Prime and G. M. Whitesides, *J. Am. Chem. Soc.*, 1993, **115**, 10714.
4 P. A. DiMilla, *J. Am. Chem. Soc.*, 1994, **116**, 2225.
5 A. Kumar, H. A. Biebuyck, N. L. Abbott and G. M. Whitesides, *J. Am. Chem. Soc.*, 1992, **114**, 9188.
6 A. Ulman, *An Introduction to Ultrathin Organic Films. Academic Press*, San Diego, CA, 1991.
7 G. Carson and S. Granick, *J. Appl. Polym. Sci.*, 1989, **37**, 2767.
8 C. R. Kessel and S. Granick, *Langmuir.*, 1991, **7**, 532.
9 D. K. Schwartz, S. Steinberg, J. Israelachvili and Z. A. N. Zasadzinski, *Phys. Rev. Lett.*, 1992, **69**, 354.
10 J. Sagiv, *J. Am Chem. Soc.*, 1980, **102**, 92.
11 J. D. Le Grange, J. L. Markham and C. R. Kurjian, *Langmuir*, 1993, **9**, 1749.
12 J. B. Brzoska, I. Ben Azouz and F. Rondelez, *Langmuir*, 1994, **10**, 4367.
13 J. B. Pethica, R. Hutchings and W. C. Oliver, *Philos. Mag. A*, 1998, **48**, 593.
14 M. F. Doerner and W. D. Nix, *J. Mater. Res.*, 1986, **1**, 601.
15 W. C. Oliver and G. M. Pharr, *J. Mater. Res.*, 1992, **7**, 1564.
16 T. Sawa, Y. Akiyama, A. Shimamoto and K. Tanaka, *J. Mater Res.*, 1999, **14**, 2228.
17 J. J. Vlassak and W. D. Nix, *J. Mech. Phys. Solids*, 1994, **42**, 1223.
18 G. A. Carson and S. Granick, *J. Mater. Res.*, 1990, **5**, 1745.
19 S. R. Wasserman, Y. T. Tao and G. M. Whitesides, *Langumuir*, 1989, **5**, 1074.
20 T. Nakagawa, K. Ogawa and T. Kurumizawa, *Langmuir*, 1994, **10**, 525.
21 E. W. van der Vegte and G. Hadziioannou, *J. Phys. Chem. B*, 1997, **101**, 9563.
22 D. V. Vezenov, A. Noy, L. F. Rosznyai and C. M. Lieber, *J. Am. Chem. Soc.*, 1997, **11**, 2006.
23 D. A. Smith, M. L. Wallwork, J. Zhang, J. Kirkham, C. Robinson, A. Marsh and M. Wong, *J. Phys. Chem. B*, 2000, **104**, 8862.
24 L. E. McNeil and M. Grimsdith, *J. Phys. Condens. Matter*, 1993, **5**, 1681.
25 M. P. Shemkumas and W. T. Petuskey, *Mat. Res. Soc. Symp. Proc.*, 1998, **552**, 275.